Heat content variability in the tropical Indian Ocean during second pre-INDOEX campaign (boreal winter 1996–1997)

E. P. Rama Rao, V. Ramesh Babu* and L. V. G. Rao
Physical Oceanography Division, National Institute of Oceanography, Dona Paula, Goa 403 004, India

Surface meteorological data and upper ocean temperature profiles are obtained on-board ORV *Sagar Kanya* (cruise 120) during the second pre-INDOEX Campaign (December 1996–January 1997) for evaluating the north–south variability of surface heat fluxes and upper oceanic heat content. Heat content in upper 200 m decreased southward by 50×10^8 Jm^{-2} along the ship's track. There is a net heat loss on either side of the equator with a marginal gain at the equator. In the vicinity of the Inter-Tropical Convergence Zone around 8°S where sea surface temperature is maximum, the heat content is conspicuously low, suggesting the divergence regime in the water column (0–200 m) due to a shear between southern equatorial and equatorial counter currents.

INDIAN Ocean Experiment (INDOEX), an international research programme, was planned for January through March 1999 over the tropical Indian Ocean in order to understand the relative roles of aerosols and clouds in the atmospheric radiative transfers and thereby the climatic changes. During the boreal winter, air masses rich in aerosol content from the Indian subcontinent move southward and meet the pristine air of the southern hemisphere in the vicinity of ITCZ. Two pre-INDOEX and one First Field Phase (FFP 98) campaigns were already conducted on-board Indian research vessel ORV *Sagar Kanya* prior to the main INDOEX (intensive field phase) programme. During the second pre-INDOEX campaign on-board ORV *Sagar Kanya* (cruise SK-120) in northern winter of 1996–1997, the N–S tracks of the cruise were used to study the N–S variability of parameters relevant to INDOEX studies. The influence of the upper ocean on the energetics of the marine boundary layer is determined by the oceanic heat content and mixed layer characteristics. The atmospheric boundary layer in ITCZ is also sensitive to the air–sea heat fluxes. In this paper, the thermal structure in the upper 225 m water column is investigated during the ship's south-bound journey from Goa to the Central Indian Ocean Basin. The N–S variability of heat content and various surface heat fluxes are studied.

*For correspondence. (e-mail: ocean@bcgoa.ernet.in)

Data and methods

Figure 1 shows the locations of the hydrographic station where the data on upper ocean thermohaline structure (0–225 m) are obtained with the help of conductivity-temperature–depth (CTD) probe (make, Seabird Electronics Inc, and model SBE-11 Plus). The resolution and accuracy limits of this instrument are 0.001% and 0.15% of full scale for pressure, 0.0002°C and 0.002°C for temperature and 0.0004 PSU and 0.003 PSU for salinity. Also, surface meteorological observations (surface winds, atmospheric pressure, air temperature humidity and cloud amount) are taken at 3 hourly

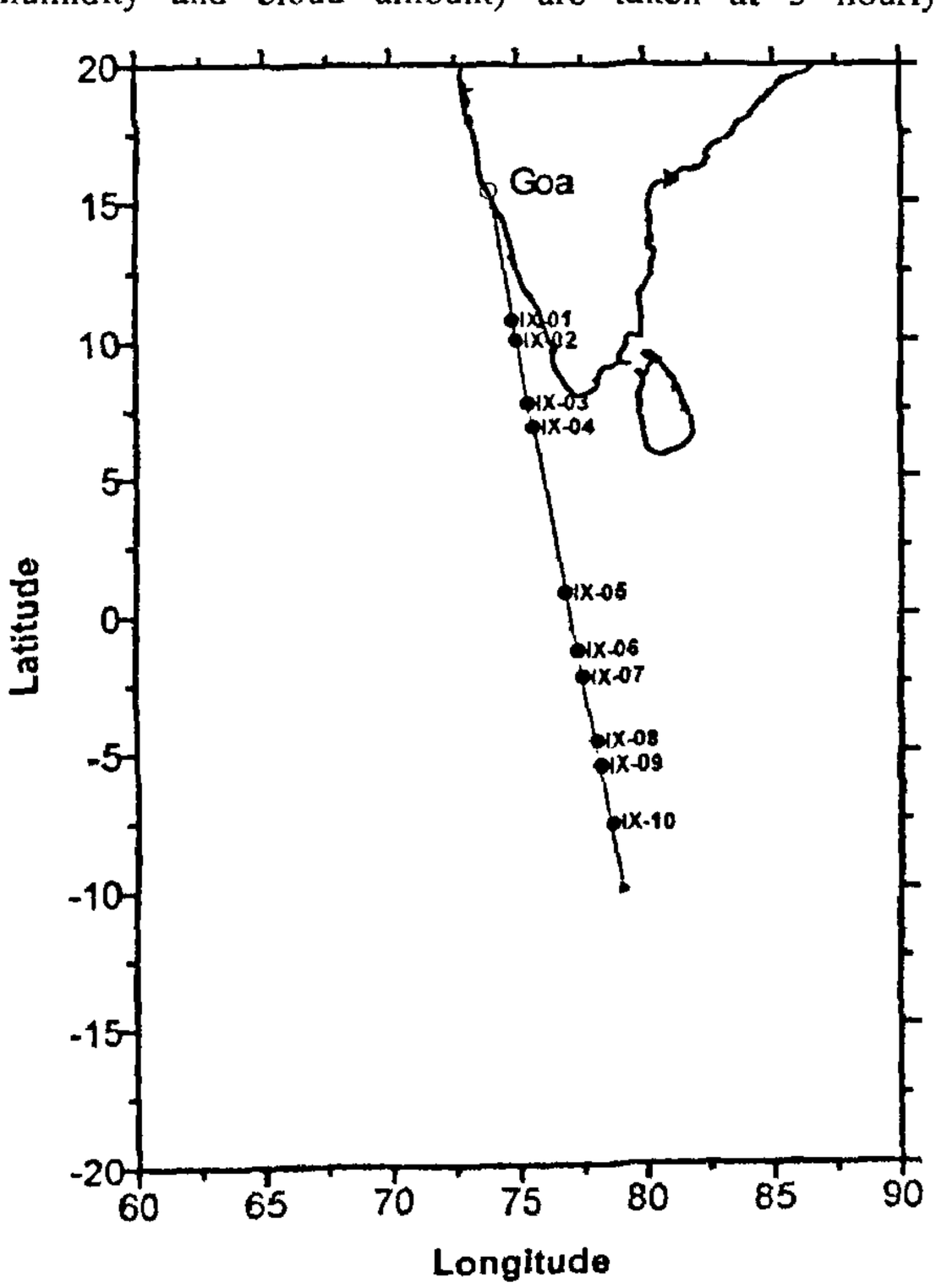

Figure 1. Location of conductivity–temperature–depth stations.

intervals during the observational period (29 December 1996 through 5 January 1997). The raw CTD data were processed using Seabird's software (Seasoft).

The heat content (Hc) of the upper water column is estimated from the following equation:

$$Hc = \rho C_p \int_0^D T \, dz,$$

where ρ is the mean density of seawater; C_p is the specific heat of sea water at constant pressure; T is the mean temperature of the layer of thickness dz; and D is the total length of the water column considered.

The various heat fluxes, i.e. latent heat flux (Q_e), sensible heat flux (Q_h) and effective back radiation (Q_b) are computed using the bulk aerodynamic formulae[1]:

$$Q_e = \rho_a C_e L_e (q_s - q_a) U_a,$$

$$Q_h = \rho_a C_{pa} C_h (T_s - T_a) U_a,$$

$$Q_b = [\varepsilon\sigma T_s^4 (0.39 - 0.05\, e_a^{1/2}) + 4\varepsilon\sigma T_s^3 (T_s - T_a)] (1 - 0.7N),$$

where ρ_a is the air density; C_e is the turbulence transfer coefficient for evaporation; L_e is the latent heat of vaporisation; C_{pa} is the specific heat capacity of air at constant pressure; C_h is the turbulence transfer coefficient for heat; T_s is the sea surface temperature; T_a is the air temperature at height 10 m; U_a is the wind speed at height 10 m; q_s is the specific humidity of saturated air at the sea surface temperature; q_a is the specific humidity of air at height 10 m; e_a is the water vapour pressure at height 10 m from sea surface; ε is the emissivity of the sea surface; σ is the Stefan–Boltzmann's constant and N is the daytime-averaged cloud amount in tenths.

The daily averaged short-wave radiation (Q_s) reaching the sea surface is estimated[2] and corrected subsequently for cloud conditions[3]. Assuming that the sea surface albedo (α) is 0.06 (ref. 4), the net heat flux (Q_n) at the sea surface is computed using the following formula:

$$Q_n = Q_s(1-\alpha) - (Q_b + Q_e + Q_h).$$

The thickness of the mixed layer is calculated following Colborn's procedure[5]. The depth–temperature profiles are inspected to locate two shallowest points across which a temperature difference of at least 0.5°C is recorded. The line between the two points is linearly extrapolated to meet an imaginary vertical line which is parallel to the depth axis and passes through the value of sea surface temperature. The depth of the intersection of these two lines then is the mixed layer thickness.

Results and discussion

Figure 2 presents the distribution of various surface meteorological parameters along the cruise track. These N–S variabilities in general show maximum SST (~ 29.0°C) around 8°S in association with lower surface atmospheric pressure and larger cloud amounts. Further, the surface air mass is more humid over the southern hemisphere than over the northern hemisphere, with the ITCZ region

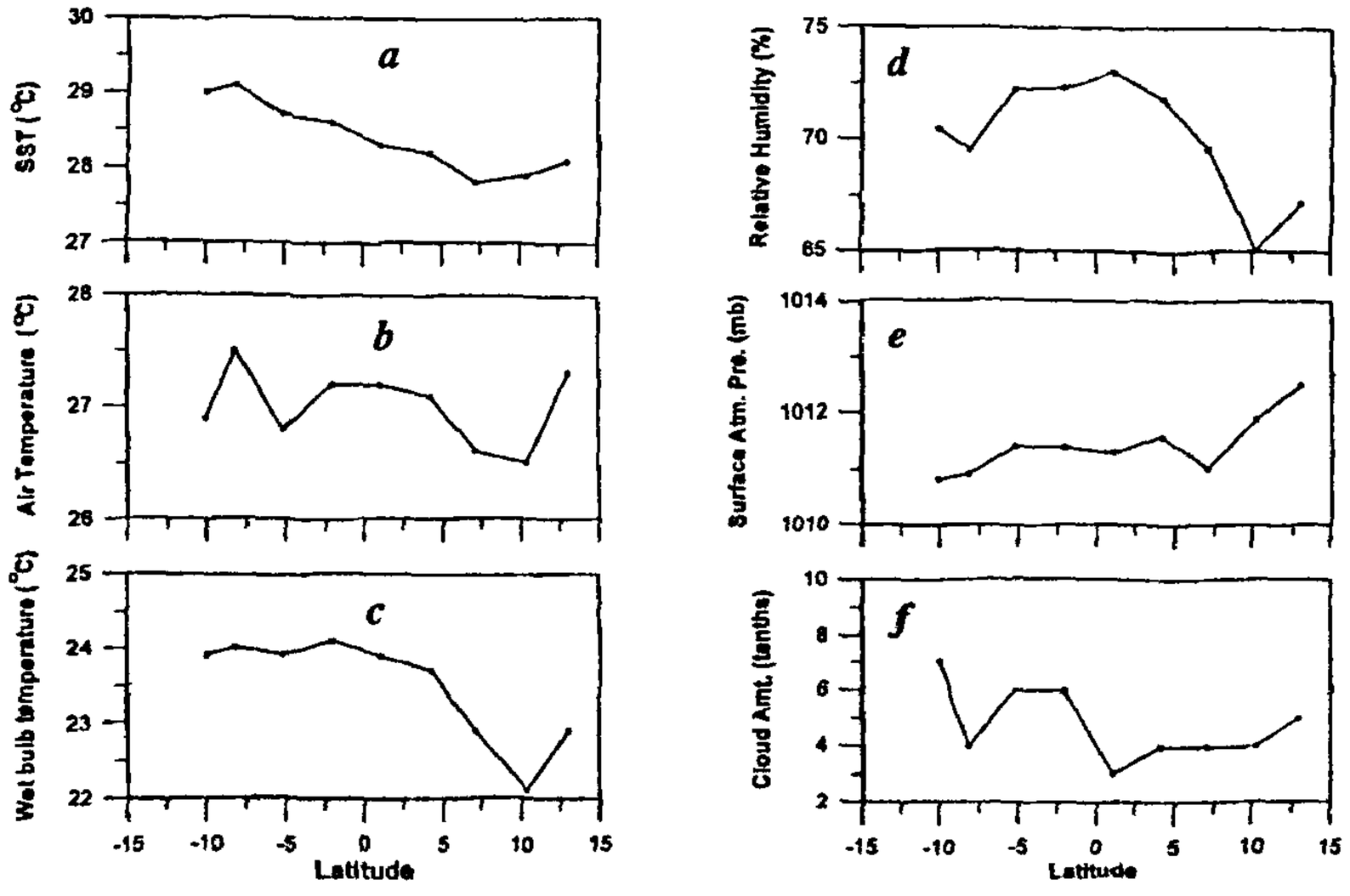

Figure 2. Distribution of surface meteorological parameters. *a*, SST (°C); *b*, Air temperature (°C); *c*, Wet bulb temperature (°C); *d*, Relative humidity (%); *e*, Surface atmospheric pressure (mb); and *f*, Cloud amount (tenths) along the cruise track.

located around 8°S. From the wind field along the cruise track (Figure 3) from Goa to the ITCZ, one could clearly see the anti-clockwise rotation in the wind direction across the equator as the winds blow mostly from N to W direction in the southern hemisphere in contrast to the north-easterly winds in the northern hemisphere.

The N–S variations of various surface heat fluxes are presented in Figure 4. The short wave radiation absorbed at the sea surface (Q_s) shows an increasing southerly trend during the study period (increased by about 100 Wm^{-2} from 14°N to 10°S). The maximum Q_s coincides with maximum SST at around 8°S. The latent heat flux (Q_e) is conspicuously low around the equator mainly because of weak winds. On the other hand, the effective back radiation (Q_b) and sensible heat flux (Q_h) show less variation from north to south. These distributions in general give rise to a net influx (positive) of heat into the sea around the equator and a net outflux (negative) of heat from the sea towards the atmosphere on either side of the equator. Thus, Q_e seems to determine the direction of net surface heat flux during the period of the present study. Climatologically during January, it is seen that both Q_e and the radiation balance ($Q_s - Q_b$) are varying in opposite directions as one proceeds from the north to 10°S resulting in negligible surface heat exchange around 10°N, since the sensible heat flux (Q_h) is normally one order less than these fluxes. North of 10°N over the Arabian Sea, Q_e is excessive over the radiation balance, and south of this latitude, the radiation balance overtakes Q_e (ref. 6). These N–S distributions of Q_e and $Q_s - Q_b$ thus cause an increasing trend in the net oceanic heat gain towards ITCZ. Q_e during this pre-INDOEX campaign compares to the climatic mean (100 Wm^{-2}) only in the equatorial region (5°N to 5°S) where the winds are in agreement with the mean values of 2–4 ms^{-1} as shown in the climatic atlas of Hastenrath and Lamb[7]. However, along the cruise track – except in equatorial region – the surface winds are strong (10 ms^{-1}) as compared to climatic mean values which results in higher evaporation and thereby a net heat loss to the atmosphere from the ocean.

The heat content in the upper 50 m layer varies narrowly between 55×10^8 Jm^{-2} and 60×10^8 Jm^{-2} except at 8°S where it is decreased to 52×10^8 Jm^{-2} (Figure 5). The effect of maximum sea surface temperature at 8°S is not reflected in the 0–50 m layer. The N–S variation of heat content is distinctively different in upper 50 m layer as compared to those in the subsurface layers, viz. 50–100 m, 100–150 m and 150–200 m. The southward decreasing trend in heat content is evident in the 50–100 m layer. However, in 100–150 m and 150–200 m

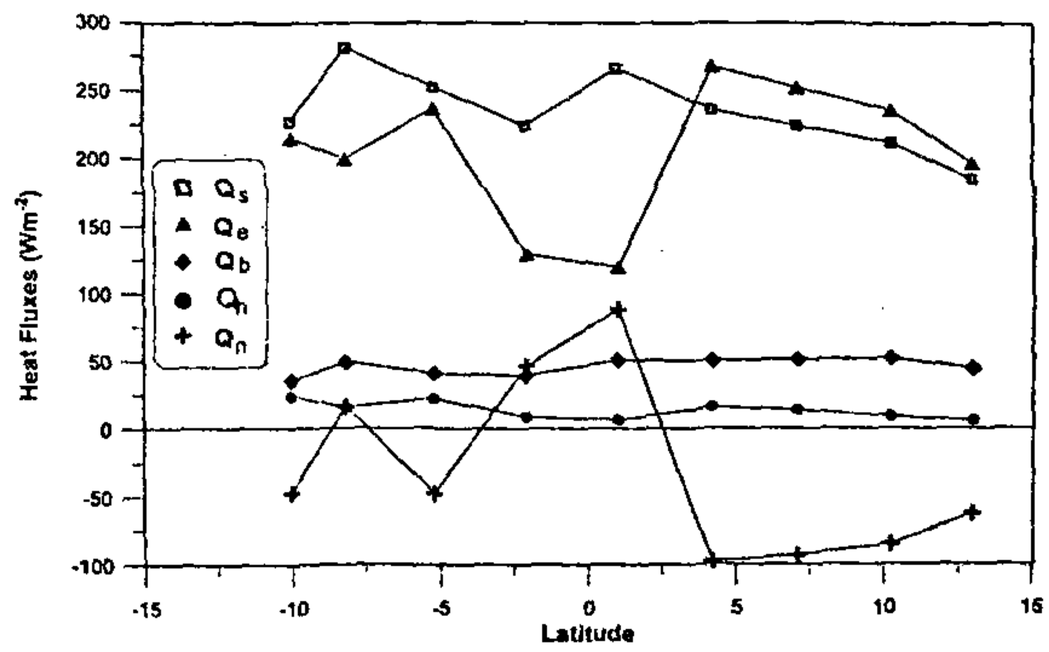

Figure 4. North–south variation of surface heat fluxes ($W\,m^{-2}$): shortwave radiation (Q_s), latent heat flux (Q_e), effective back radiation (Q_b), sensible heat flux (Q_h) and net heat flux (Q_n).

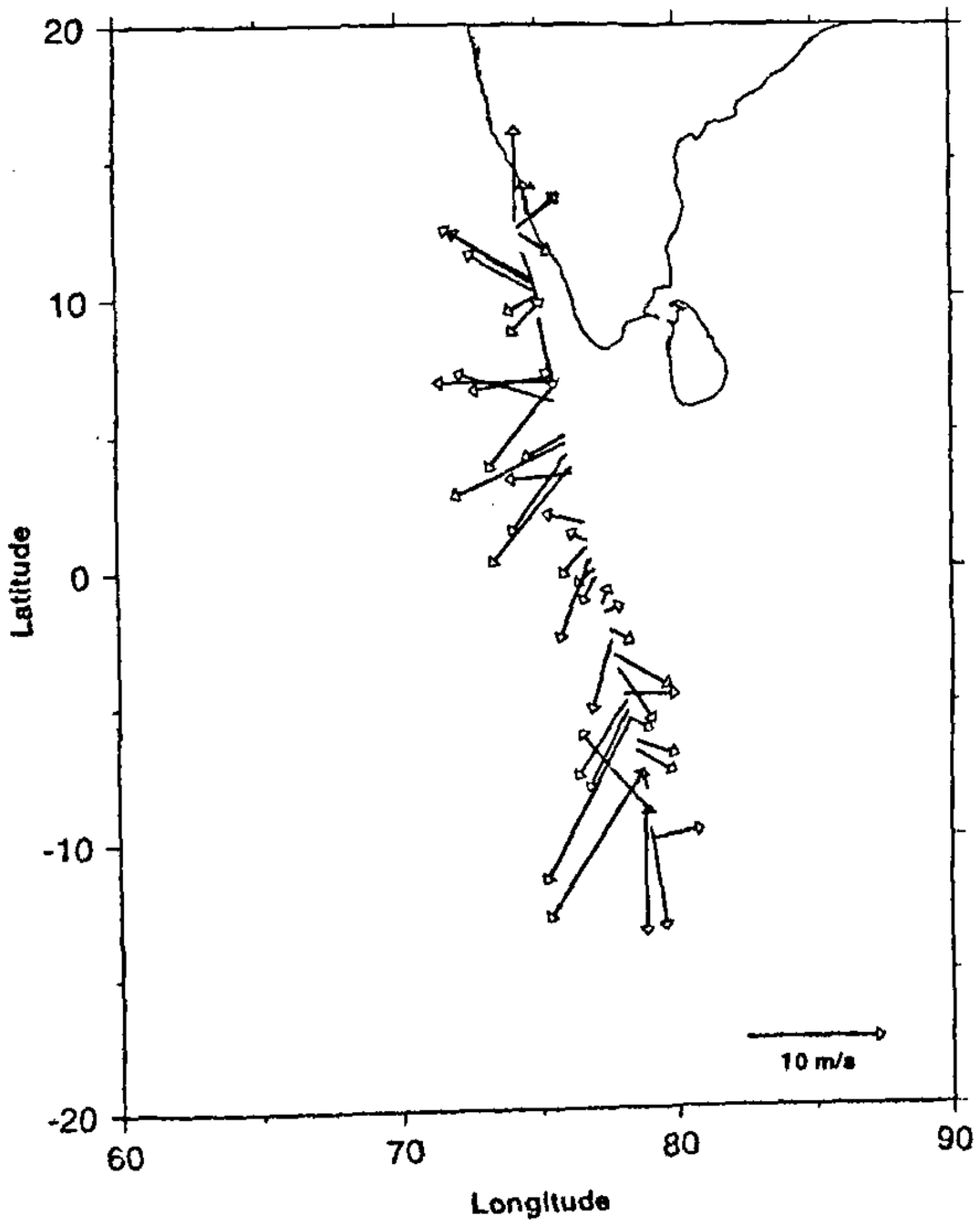

Figure 3. Distribution of surface winds along the cruise track.

Figure 5. North–south variation of heat content ($\times 10^8$ Jm^{-2}) in different layers.

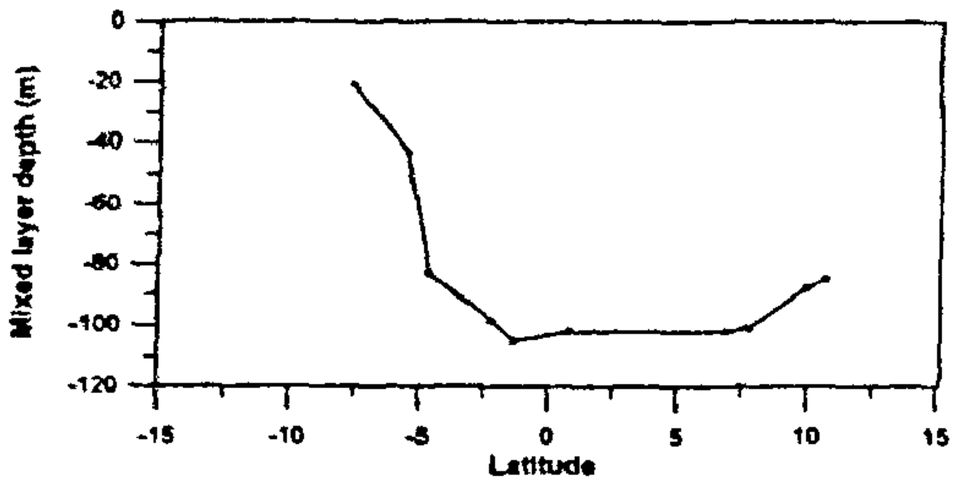

Figure 6. North–south variation of mixed layer thickness (m).

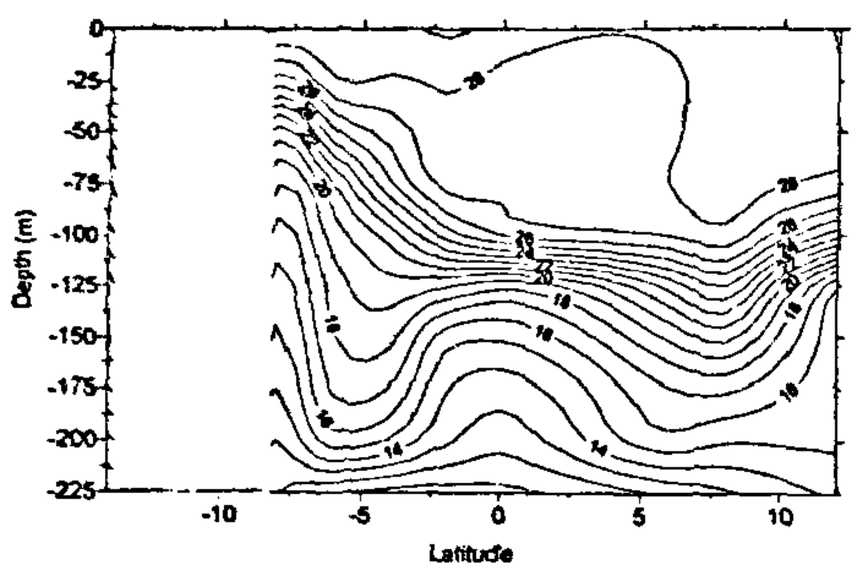

Figure 7. Vertical structure of temperature (°C) in the upper water column (0–225 m depth) along the ship's transect.

layers, there is bimodal distribution in which heat content varies with notable peaks around 8°N and 6°S respectively.

Interestingly the mixed layer is thinnest (~ 20 m) at 8°S (Figure 6). At this shallowest thermocline region, the sea surface temperature is high and the winds are found to be relatively strong (~ 13 ms^{-1}) as compared to those over the equator. An examination of thermal structure indicates a distinct uplift of thermocline to 8°S from the equator in the upper 100 m (Figure 7). The lower thermocline region exhibits two troughs present around 8°N and 6°S, respectively, resulting in the bimodal distribution of heat content as shown earlier. Between these troughs, a ridge is interspaced around the equator. This thermal structure suggests the thermocline's response to the divergence and convergence fields associated with the zonal current systems in the tropical Indian Ocean. The salinity distribution (Figure 8) in the upper 225 m along the cruise track shows different regimes of water masses being carried by the zonal currents. Around 5°N, the water mass in the upper 50 m is low saline (< 34.58 PSU) because of the north equatorial current (NEC) carrying low saline waters from east to west during boreal winter. However, near the equator the salinity is maximum (> 34.76 PSU) on account of high salinity waters carried west to east by the equatorial counter current (ECC). Farther south near 8°S, the surface salinity decreases to 34.70 PSU on account of the influence of the south equatorial current (SEC) which carries low salinity water from east to west. The ridge in

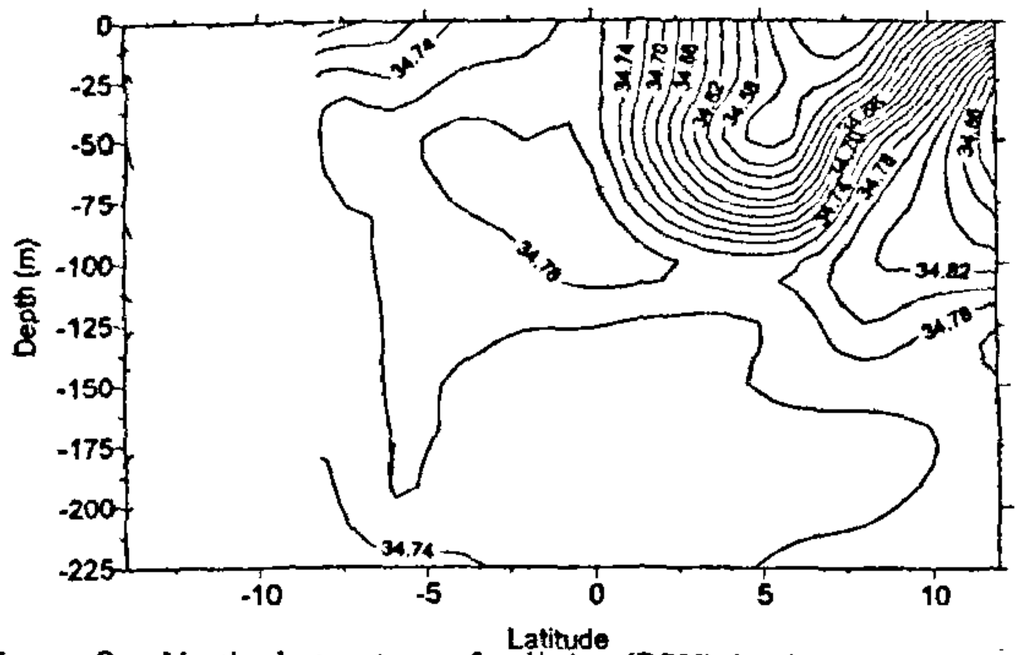

Figure 8. Vertical structure of salinity (PSU) in the upper water column (0–225 m depth) along the ship's transect.

the thermocline at 8°S is attributed to clockwise rotating gyre bounded on the south by the SEC and on the north by the ECC during boreal winter[8]. The trough in the thermocline region at 8°N is related to convergence associated with Lakshadweep High[9]. The present study indicates that the mixed layer thickness in the tropical Indian Ocean is influenced by the vergence fields associated with upper ocean circulation patterns.

Further studies involving directly measured currents in the upper ocean along the cruise track are needed to assess the role of the circulation in the heat content variability. In the forthcoming main INDOEX (or Intensive Field Phase) cruise scheduled during northern winter 1999, direct current measurements using acoustic doppler current profile (ADCP) form an important component of the oceanographic programme.

1. Stevenson, J. W., *Computation of Heat and Momentum Fluxes at the Sea Surface During the Hawaii to Tahiti Shuttle Experiment*, Univ. Hawaii, Honolulu, Hawaii, 1982.
2. Seckel, G. R. and Beaudry, F. H., *Trans. Am. Geophys. Union*, 1973, **54**, 1114.
3. Reed, R. K., *J. Geophys. Res.*, 1977, **7**, 482–485.
4. Payne, R. E., *J. Atmos. Sci.*, 1972, **29**, 959–970.
5. Colborn, J. G., *The Thermal Structure of the Indian Ocean*, The University Press of Hawaii, Honolulu, 1975.
6. Hastenrath, S. and Lamb, P. J., *Climatic Atlas of the Indian Ocean, Part II: The Oceanic Heat Budget*, The University of Wisconsin Press, Wisconsin, 1979.
7. Hastenrath, S. and Lamb, P. J., *Climatic Atlas of the Indian Ocean, Part I: Surface Climate and Atmospheric Circulation*, The University of Wisconsin Press, Wisconsin, 1979.
8. Molinari, R. L., Olson, D. and Reverdin,G., *J. Geophys. Res.*, 1990, **95**, 7217–7238.
9. Shankar, D. and Shetye, S. R., *J. Geophys. Res.*, 1997, **102**, 12551–12562

ACKNOWLEDGEMENTS. We thank Dr E. Desa, Director NIO, and Dr A. P. Mitra, Chairman, INDOEX National Steering Committee, for their support and encouragement. We also thank the Department of Ocean Development (Government of India) for ORV *Sagar Kanya*. One of the authors (E.P.R.) acknowledges the Department of Ocean Development for the Fellowship under MARSIS Seatruth Collection Project and Ocean Observing System Programme.